Experimental Demonstration of Linear Least Squares-based Longitudinal Power Monitoring over a Raman-amplified C+L Link

Experimental Demonstration of Linear Least Squares-based Longitudinal Power Monitoring over a Raman-amplified C+L Link

Lorenzo Andrenacci[(1)], Stefano Straullu[(2)], Antonino Nespola[(2)], Gabriella Bosco[(1)], Pierluigi Poggiolini[(1)], Stefano Piciaccia[(3)], and Dario Pilori[(1)]

[(1)] DET, Politecnico di Torino, Torino, Italy. lorenzo.andrenacci@polito.it
[(2)] LINKS Foundation, Torino, Italy.
[(3)] Cisco Photonics Italy S.r.l., Vimercate (MB), Italy.

Abstract *We present the first experimental demonstration of a linear least squares-based longitudinal power monitoring algorithm over a C+L link with full backward Raman amplification, transmitting 64-GBaud PDM-QPSK signals over 9x60-km spans of SMF.*

Introduction

Monitoring the optical performance is essential for ensuring the dependable function and efficient administration of contemporary optical networks. Indeed, meeting the demands of modern communications hinges on adaptability and substantial capacity, necessitating monitoring solutions that are both cost-effective and streamlined in complexity[1]. Among those, longitudinal power monitoring (LPM)[2] is a powerful technique that allows the estimation of the power profile of the signal along the link, without requiring additional information at the receiver. LPM has been successfully demonstrated to estimate not only the power, but also additional system parameters, such as polarization-dependent loss[3],[4], fiber types[5] and gain spectra of optical amplifiers[6]. In particular, linear least squares (LLS)-based LPM[7] allows for the direct estimation of the absolute optical power. This enables the use of LPM not only for monitoring, but also for the design and optimization of a live network[8],[9], aided by simplified physical-layer-aware models[10].

In recent years, there have been several extensive experimental demonstrations of LPM. A particularly challenging scenario is the ultra-wide band (UWB) scenario[11] (i.e., beyond the C-band), where the choice of the amplification scheme is particularly important[12]. In fact, doped fiber amplifiers (such as the EDFA) cannot provide gain for the entire WDM comb, thus requiring multiple parallel amplifiers, which increase the cost and the complexity of the system. Therefore, there are two main solutions to amplify a UWB system with a single amplifier: Raman and semiconductor optical amplifiers (SOAs)[12]. While some recently-developed SOAs can achieve a significant gain over $100+$ nm of bandwidth, they still have issues, such as a high Noise Figure and Polarization-Dependent Gain. On the other hand, Raman amplification can achieve amplification over a wide bandwidth with a small noise figure[13]. However, it is particularly difficult to design and optimize a Raman-amplified UWB link, also due to the interplay with inter-channel stimulated Raman scattering (ISRS)[14]. Therefore, an accurate live monitoring of the per-channel power profile is critical for the operation and optimization of a Raman-amplified UWB transmission system.

Some simulative and experimental demonstrations of LPM in UWB scenarios have already been published, involving the monitoring of EDFA spectral gain, potential anomalies (e.g., gain tilt and narrowband gain compression)[15],[16] and ISRS[17]. However, in[15],[16] the authors resorted to a correlation-based LPM method[18], which requires both CD pre-distortion and a calibration procedure[19] to retrieve the real optical power and perform all the aforementioned operations. Moreover, the link distance was limited, up to $280\,\mathrm{km}$, and none of them employed a full Raman-based amplification scheme. In fact, LPM has only been demonstrated in hybrid Raman-EDFA transmission scenarios, in simulation, for very short distances and few WDM channels[8], and in an experiment, considering just a single C-band transmission[6]. In this work, we present the application of LLS-based LPM over a full backward Raman-amplified C+L band system, composed of 9×60-km spans of G.652 single mode fiber (SMF). We show that, at all power levels, we can obtain power profiles that closely match the power levels measured by optical spectrum analyzers (OSAs).

Methodology

In this work, all power profiles are estimated resorting to LLS-based LPM[7]. The key idea is to reconstruct the transmitted signal $\mathbf{A}_{\mathrm{ref}}[0,n]$ at the receiver side and virtually propagate it according to the first-order enhanced regular perturbation (eRP1) model[20]. This allows to approximate the propagated signal as $\mathbf{A}_{\mathrm{ref}}[L,n] \simeq \mathbf{A}_{\mathrm{ref},0}[L,n] + \mathbf{A}_{\mathrm{ref},1}[L,n]$, where L is the length of the link and n is the discrete-time index. The same approximation can be made for the actual received

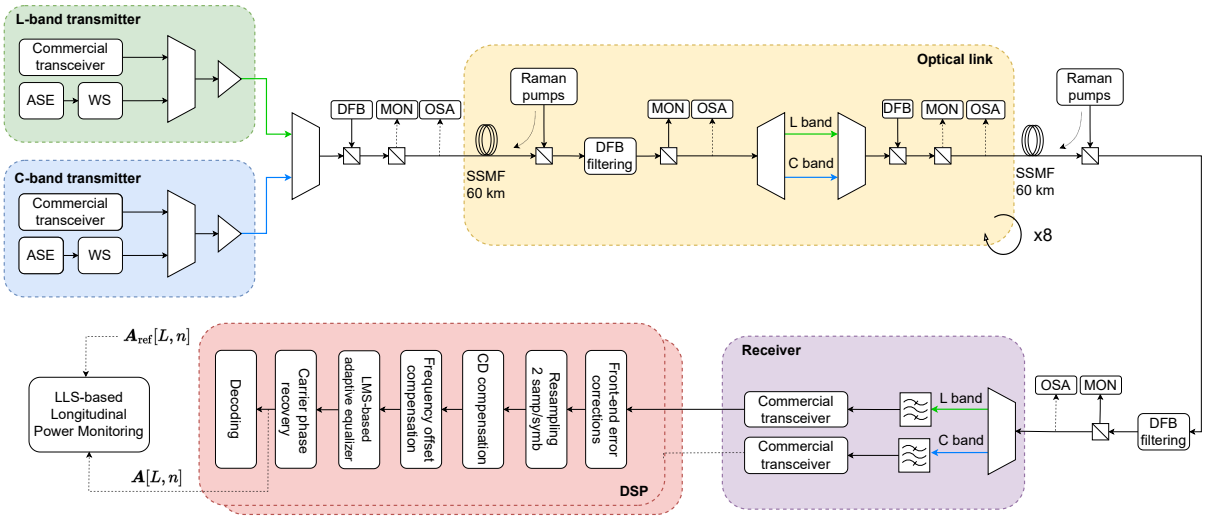

Fig. 1: Experimental setup. WS: WaveShaper; DFB: distributed feedback laser; MON: monitor;

signal, i.e., $\mathbf{A}[L,n] \simeq \mathbf{A}_0[L,n] + \mathbf{A}_1[L,n]$. It is then possible to demonstrate that the corresponding power profile $\boldsymbol{\gamma}' = \frac{8}{9}\gamma\boldsymbol{P}$ can be estimated in closed-form as:

$$\hat{\boldsymbol{\gamma}}' = \left(\mathrm{Re}\left[\mathbf{G}^{\dagger}\mathbf{G}\right]\right)^{-1}\mathrm{Re}\left[\mathbf{G}^{\dagger}\mathbf{A}_1[L,n]\right] \qquad (1)$$

where $\mathbf{G}$ is a matrix including all the terms for the eRP1 approximation, computed starting from $\mathbf{A}_{\mathrm{ref}}[0,n]$.

Experimental setup and results

The experimental setup is shown in Fig. 1. At the transmitter, two commercial transceivers (one in the C-, and one in the L-band) generate 64-GBaud PDM-QPSK signals for the channel under test (CUT). The wavelength of these transceiver was changed during the experiment to measure different WDM channels. The rest of the WDM channels were emulated with shaped ASE noise, to achieve a total of 36 channels (18 per band), spaced by 200 GHz. The spacing was set to this large value to obtain accurate channel-resolved in-line OSNR measurements with the OSA, and to potentially allow a large per-channel transmit power. Two booster EDFA amplifiers set the total launch power, which is adjusted to 0, 4 and 8 dBm per channel, with a flat power profile. The WDM signal is then transmitted to a set of 9 spans, each made by 60 km of G.652 SMF, and amplified with 5 counter-propagating Raman pumps, whose wavelength and power is shown in Tab. 1.

Tab. 1: Raman pumps configuration

Wavelength (nm)	Power (mW)
1423.81	306
1435.29	280
1450.25	178
1465.91	121
1494.82	173

The C-band and L-band WDM signals are combined at the beginning of each span and separated at the exit. A set of monitors and an OSA are used to accurately measure the power of each channel and determine the channel-resolved OSNR at both the input and output of each span. No gain equalization is inserted in the system: this creates strong differences in the per-channel power, which allows to test the LPM algorithm in different scenarios. Note that the light generated by a distributed feedback (DFB) laser source is multiplexed to the transmitted signal. It acts as a monitor for the Raman modules in order to switch on and off the Raman pumps.

At the end of the 9^{th} span, the WDM comb is demultiplexed and received by a commercial transceiver. Instead of relying on the transceiver real time DSP implementation, we extracted the raw ADC samples, and implemented an offline DSP chain. The DSP chain is composed by a resampling at 2 sample-per-symbol, blind frequency offset compensation, CD estimation[21] and compensation, LMS-based 2×2 MIMO fractionally-spaced equalization and Viterbi-Viterbi (4-th power) phase recovery. Afterwards, the received constellation is compared to the transmitted sequence to compute the SNR.

We measured a total of 6 channels: 3 in the L band (i.e., channel 3, 9 and 15) centered at 187.06, 188.26 and $189.46\,\mathrm{THz}$ and 3 in the C band (i.e., channel 3, 9 and 15) centered at 191.90, 193.10 and $194.30\,\mathrm{THz}$. For each measurement, we captured 25 sequences of 2^{17} samples from the ADCs of the card, sampled at 96 Gs/s. LLS-based LPM was then applied to the captured sequences with a spatial resolution $\Delta z = 2\,\mathrm{km}$ and the resulting 25 profiles were averaged to reduce the estimation noise.

The following results refer to the $P_{\mathrm{ch}} = 0$ dBm transmission condition. However, they are equivalent for all the other tested scenarios.

Fig. 2(a) displays the optical power evolution in space and frequency of each measured WDM

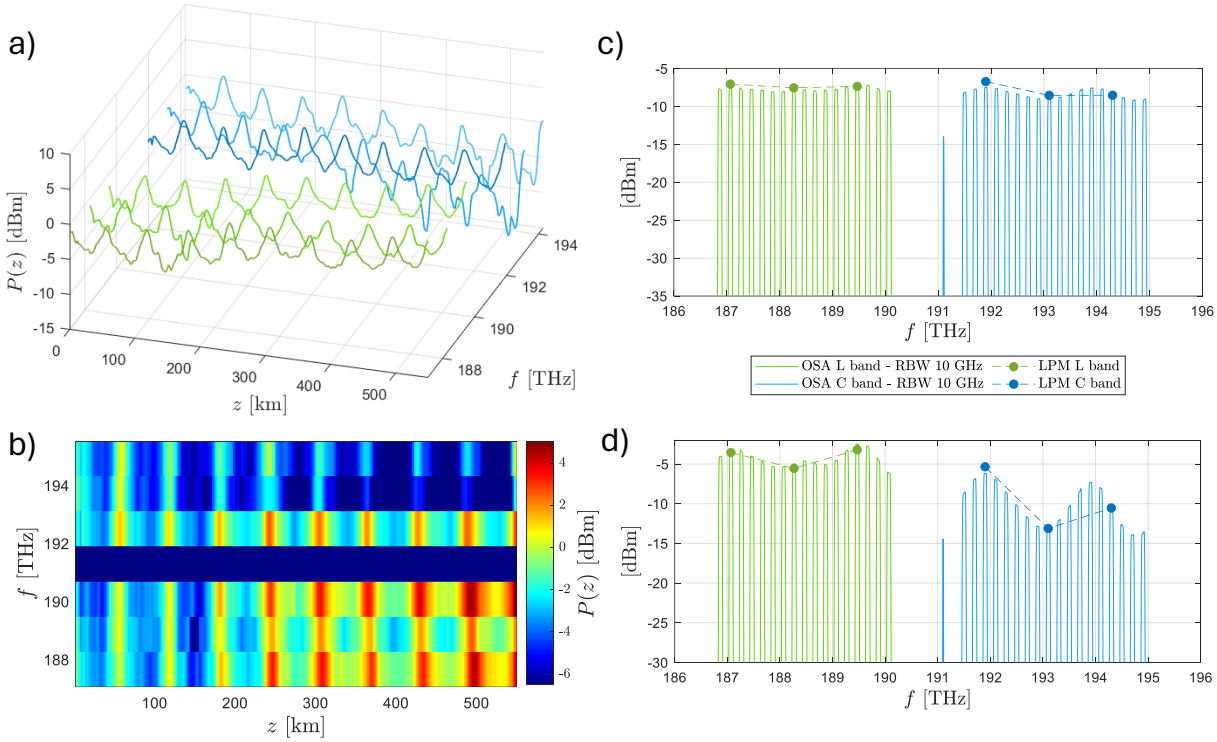

Fig. 2: a) Estimated power profiles after 25-profile averaging for the measured channels in L (green) and C (blue) bands with $P_{\mathrm{ch}} = 0$ dBm. b) Spectral and spatial optical power evolution over the link. OSA power spectrum vs. LPM power estimates at the input of the c) 3rd and d) 9th span.

channel. Note that LLS-based algorithm estimates $\boldsymbol{\gamma'} = \frac{8}{9}\gamma \boldsymbol{P}$. This implies that the knowledge of the nonlinear fiber parameter γ is required to compute the absolute optical power. Moreover, in the UWB scenario, γ has a (weak) wavelength dependence, which must be taken into account to obtain accurate results. Consequently, it was estimated using the method described in[22],[23], considering only the self-channel interference (SCI) contribution, since it is the only contribution that is used by LPM to estimate the power profile.

From the power profiles shown in Fig. 2(a) it is possible to clearly observe the effect of Raman scattering originating from both the Raman pumps and the other WDM channels. This justifies the evolution of the different profiles that exhibit a general increase in power while moving towards the L-band and create a ripple effect over the spectrum. Fig. 2(b) highlights the power intensity over the frequency-space grid and gives a better representation of this behavior. To validate the obtained results, the estimated power values are compared to the power spectra measured by the OSA at the input of each span. Since the power values from the OSA are integrated over a reference bandwidth (RBW) of $10\,\mathrm{GHz}$, the power values estimated by the LPM algorithm are also normalized with respect to this value. We report in Fig. 2(c-d) the results relative to the input power at the beginning of the 3rd and 9th spans, respectively. The estimated values are consistent with those measured by the OSA and follow the correct power evolution of the channels of interest throughout the link. In particular, at the input of the 3rd span the power spectrum is still relatively flat. However, a large ripple appears after propagation, generating a power imbalance between the measured channels. This imbalance is approximately $2\,\mathrm{dB}$ for both channels 3-9 and 9-15 in the L band, while it increases up to $8\,\mathrm{dB}$ and $3\,\mathrm{dB}$ for the same channels in the C band. In all cases, the LPM algorithm manages to capture them.

The absolute estimation error between the rescaled power values from LPM and those from OSA is also computed. At the beginning of the 3rd span the errors are always below $0.77\,\mathrm{dB}$, with a mean value equal to $0.43\,\mathrm{dB}$. The maximum error is slightly higher for the 9th span, i.e., $0.83\,\mathrm{dB}$, but the mean value remains $0.43\,\mathrm{dB}$. Moreover, this strongly suggests that the entire LPM profile would match with the profile computed with an analytical solution of the Raman equations.

Conclusions

In this work, we apply LLS-based longitudinal power monitoring to a C+L band transmission system composed of a 9×60 km SMF link with full Raman amplification. We show that LPM is able to accurately monitor (with a maximum absolute error $< 0.83\,\mathrm{dB}$) the power evolution of different channels, both in the C- and in the L-band, by comparing its predictions with measurements obtained with OSAs. This information can then be used for the design and the optimization of such systems.

Acknowledgements

This work was carried out in the PhotoNext Center at Politecnico di Torino (www.photonext.polito.it) under a research program with Cisco Photonics. It was also partially sponsored by the European Union under the Italian National Recovery and Resilience Plan (NRRP) of NextGenerationEU, partnership on 'Telecommunications of the Future' (PE00000001 - program 'RESTART').

References

[1] F. N. Hauske, M. Kuschnerov, B. Spinnler, and B. Lankl, "Optical performance monitoring in digital coherent receivers", *J. Lightw. Technol.*, vol. 27, no. 16, pp. 3623–3631, 2009. DOI: 10.1109/JLT.2009.2024960.

[2] T. Sasai, M. Takahashi, R. Kaneko, Y. Sone, M. Nakamura, and E. Yamazaki, "Recent advances in digital longitudinal monitoring of fiber-optic link", in *Optical Fiber Communication Conference (OFC) 2024*, 2024, W1B.3.

[3] M. Takahashi, T. Sasai, E. Yamazaki, and Y. Kisaka, "DSP-based PDL estimation and localization in multi-span optical link using least squares-based longitudinal power monitoring", in *2023 Opto-Electronics and Communications Conference (OECC)*, 2023, pp. 1–6. DOI: 10.1109/OECC56963.2023.10209964.

[4] L. Andrenacci, G. Bosco, and D. Pilori, "PDL localization and estimation through linear least squares-based longitudinal power monitoring", *IEEE Photon. Technol. Lett.*, vol. 35, no. 24, pp. 1431–1434, 2023. DOI: 10.1109/LPT.2023.3331110.

[5] M. Eto, K. Tajima, K. Sone, *et al.*, "Fibre type identification based on power profile estimation", in *49th European Conference on Optical Communications (ECOC 2023)*, vol. 2023, 2023, pp. 127–130. DOI: 10.1049/icp.2023.1888.

[6] T. Sasai, M. Nakamura, E. Yamazaki, S. Yamamoto, H. Nishizawa, and Y. Kisaka, "Digital longitudinal monitoring of optical fiber communication link", *J. Lightw. Technol.*, vol. 40, no. 8, pp. 2390–2408, Apr. 2022. DOI: 10.1109/JLT.2021.3139167.

[7] T. Sasai, M. Takahashi, M. Nakamura, E. Yamazaki, and Y. Kisaka, "Linear least squares estimation of fiber-longitudinal optical power profile", *J. Lightw. Technol.*, vol. 42, no. 6, pp. 1955–1965, 2024. DOI: 10.1109/JLT.2023.3327760.

[8] I. Kim, O. Vassilieva, S. Oda, P. Palacharla, and T. Hoshida, "Nonlinear SNR estimation based on power profile estimation in hybrid Raman-EDFA link", in *Optical Fiber Communication Conference (OFC) 2024*, 2024, Th1F.6.

[9] H. Nishizawa, G. Borraccini, T. Sasai, *et al.*, *Semi-automatic line-system provisioning with integrated physical-parameter-aware methodology: Field verification and operational feasibility*, 2024. arXiv: 2403.16281 [eess.SY].

[10] V. Curri, "GNPy model of the physical layer for open and disaggregated optical networking [invited]", *Journal of Optical Communications and Networking*, vol. 14, no. 6, pp. C92–C104, 2022. DOI: 10.1364/JOCN.452868.

[11] T. Hoshida, V. Curri, L. Galdino, *et al.*, "Ultrawideband systems and networks: Beyond C+L-band", *Proc. IEEE*, vol. 110, no. 11, pp. 1725–1741, 2022. DOI: 10.1109/JPROC.2022.3202103.

[12] J. Renaudier, A. Napoli, M. Ionescu, *et al.*, "Devices and fibers for ultrawideband optical communications", *Proc. IEEE*, vol. 110, no. 11, pp. 1742–1759, 2022. DOI: 10.1109/JPROC.2022.3203215.

[13] W. S. Pelouch, "Raman amplification: An enabling technology for long-haul coherent transmission systems", *J. Lightw. Technol.*, vol. 34, no. 1, pp. 6–19, 2016. DOI: 10.1109/JLT.2015.2458771.

[14] M. Cantono, A. Ferrari, D. Pilori, E. Virgillito, J. L. Augé, and V. Curri, "Physical layer performance of multi-band optical line systems using Raman amplification", *J. Opt. Commun. Netw.*, vol. 11, no. 1, A103–A110, Jan. 2019. DOI: 10.1364/JOCN.11.00A103.

[15] M. Sena, R. Emmerich, B. Shariati, *et al.*, "DSP-based link tomography for amplifier gain estimation and anomaly detection in C+L-band systems", *J. Lightw. Technol.*, vol. 40, no. 11, pp. 3395–3405, 2022.

[16] M. Sena, P. Hazarika, C. Santos, *et al.*, "Advanced DSP-based monitoring for spatially resolved and wavelength-dependent amplifier gain estimation and fault location in C+L-band systems", *J. Lightw. Technol.*, vol. 41, no. 3, pp. 989–998, 2023.

[17] R. Kaneko, T. Sasai, F. Hamaoka, M. Nakamura, and E. Yamazaki, "Fiber longitudinal monitoring of inter-band-SRS-induced power transition in S+C+L WDM transmission", in *2024 Optical Fiber Communications Conference and Exhibition (OFC)*, 2024, W1B.4.

[18] T. Tanimura, S. Yoshida, K. Tajima, S. Oda, and T. Hoshida, "Fiber-longitudinal anomaly position identification over multi-span transmission link out of receiver-end signals", *J. Lightw. Technol.*, vol. 38, no. 9, pp. 2726–2733, May 2020. DOI: 10.1109/JLT.2020.2984270.

[19] A. May, F. Boitier, E. Awwad, P. Ramantanis, M. Lonardi, and P. Ciblat, "Receiver-based experimental estimation of power losses in optical networks", *IEEE Photon. Technol. Lett.*, vol. 33, no. 22, pp. 1238–1241, 2021. DOI: 10.1109/LPT.2021.3115627.

[20] P. Serena and A. Bononi, "An alternative approach to the Gaussian noise model and its system implications", *J. Lightw. Technol.*, vol. 31, no. 22, pp. 3489–3499, Nov. 2013. DOI: 10.1109/JLT.2013.2284499.

[21] C. Malouin, P. Thomas, B. Zhang, J. O'Neil, and T. Schmidt, "Natural expression of the best-match search godard clock-tone algorithm for blind chromatic dispersion estimation in digital coherent receivers", in *Advanced Photonics Congress*, Optica Publishing Group, 2012, SpTh2B.4. DOI: 10.1364/SPPCOM.2012.SpTh2B.4.

[22] M. Santagiustina, C. G. Someda, G. Vadalà, S. Combrié, and A. D. Rossi, "Theory of slow light enhanced four-wave mixing in photonic crystal waveguides", *Opt. Express*, vol. 18, no. 20, pp. 21 024–21 029, Sep. 2010. DOI: 10.1364/OE.18.021024.

[23] P. Poggiolini and M. Ranjbar-Zefreh, "Closed form expressions of the nonlinear interference for UWB systems", in *2022 European Conference on Optical Communication (ECOC)*, 2022, pp. 1–4.